Molecular Neurobiology (2019) 56:1221–1232
https://doi.org/10.1007/s12035-018-1163-0

(E)-Nicotinaldehyde O-Cinnamyloxime, a Nicotine Analog, Attenuates Neuronal Cells Death Against Rotenone-Induced Neurotoxicity

Juan Camilo Jurado-Coronel[1] · Alix E. Loaiza[2] · John E. Díaz[2] · Ricardo Cabezas[1] · Ghulam Md Ashraf[3] · Amirhossein Sahebkar[4,5,6] · Valentina Echeverria[7,8] · Janneth González[1] · George E. Barreto[1]

Received: 27 March 2018 / Accepted: 30 May 2018 / Published online: 7 June 2018

Abstract

Parkinson's disease (PD) is a neurodegenerative pathology characterized by resting tremor, rigidity, bradykinesia, and loss of dopamine-producing neurons in the pars compacta of the substantia nigra in the central nervous system (CNS) that result in dopamine depletion in the striatum. Oxidative stress has been documented as a key pathological mechanism for PD. Epidemiological studies have shown that smokers have a lower incidence of PD. In this aspect, different studies have shown that nicotine, a chemical compound found in cigarette, is capable of exerting beneficial effects in PD patients, but it can hardly be used as a therapeutic agent because of its inherent toxicity. Several studies have suggested that the use of nicotine analogs can have the same benefits as nicotine but lack its toxicity. In this study, we assessed the effects of two nicotine analogs, (*E*)-nicotinaldehyde O-cinnamyloxime and 3-(pyridin-3-yl)-3a,4,5,6,7,7a-hexahidrobenzo[d]isoxazole, in an in vitro model of PD. Initially, we performed a computational prediction of the molecular interactions between the nicotine analogs with the α7 nicotinic acetylcholine receptor (nAChR). Furthermore, we evaluated the effect of nicotine, nicotine analogs and rotenone on cell viability and reactive oxygen species (ROS) production in the SH-SY5Y neuronal cell line to validate possible protective effects. We observed that pre-treatment with nicotine or (E)-nicotinaldehyde O-cinnamyloxime (10 μM) improved cell viability and diminished ROS production in SH-SY5Y cells insulted with rotenone. These findings suggest that nicotine analogs have a potential protective effect against oxidative damage in brain pathologies.

Keywords Parkinson's disease · Nicotine analogs · (*E*)-nicotinaldehyde O-cinnamyloxime · Rotenone · Cell viability · Oxidative stress

Introduction

Parkinson's disease (PD) is a relatively common disorder of the Central Nervous System (CNS) that is characterized by a selective and progressive degeneration of dopaminergic neurons and the presence of Lewy bodies in the substantia nigra pars compacta, causing dopamine depletion in the striatum [1]. PD patients suffer from tremors, slowness of movements, gait

Electronic supplementary material The online version of this article (https://doi.org/10.1007/s12035-018-1163-0) contains supplementary material, which is available to authorized users.

✉ Janneth González
janneth.gonzalez@javeriana.edu.co

✉ George E. Barreto
gsampaio@javeriana.edu.co

[1] Departamento de Nutrición y Bioquímica, Facultad de Ciencias, Pontificia Universidad Javeriana, Bogotá, D. C., Colombia

[2] Departamento de Química, Facultad de Ciencias, Pontificia Universidad Javeriana, Bogotá, D. C., Colombia

[3] King Fahd Medical Research Center, King Abdulaziz University, Jeddah 21589, Saudi Arabia

[4] Neurogenic Inflammation Research Center, Mashhad University of Medical Sciences, Mashhad, Iran

[5] Biotechnology Research Center, Pharmaceutical Technology Institute, Mashhad University of Medical Sciences, Mashhad, Iran

[6] School of Pharmacy, Mashhad University of Medical Sciences, Mashhad, Iran

[7] Facultad de Ciencias de la Salud, Universidad San Sebastián, Lientur 1457, 4030000 Concepción, Chile

[8] Bay Pines VA Healthcare System, Research and Development, Bay Pines VAHCS, 10,000 Bay Pines Blvd., Bldg. 23, Rm123, Bay Pines, FL 33744, USA

instability, and rigidity. These patients may also present functional disability, reduced quality of life, and rapid cognitive decline.

It has been shown that nicotine, and derivatives such as cotinine, exert beneficial effects in patients suffering from diseases such as PD, Alzheimer's disease, anxiety, schizophrenia, and other pathologies affecting the CNS [2–10]. Moreover, previous studies have demonstrated an inverse relationship between smoking and the risk of developing PD, an association that has been observed in more than 40 independent studies made by different researchers in the last 50 years [11, 12]. However, nicotine has the potential to cause damage to cardiovascular and gastrointestinal systems and is capable of affecting sleep cycles as well as causing addiction and dependence [11, 13]. The dose-limiting side effects emanating from an indiscriminate activation of many types of nicotinic receptors, toxicity, and addictive properties limit the application of nicotine as a therapeutic agent. For these reasons, several nicotine analogs have been developed with the aim of retaining the beneficial effects of the parent compound but lacking its toxicity [14–18].

Efforts have been made to remove reactive oxygen species (ROS) or prevent their formation as a therapeutic strategy in PD [19–21]. In this aspect, nicotine analogs could be useful in the treatment of neurodegenerative diseases through different mechanisms including stimulation of dopamine release in the striatum and activation of HIF-1a, which is related to ROS homeostasis [22, 23]. Different experimental compounds have been used in PD research, including several inhibitors of mitochondrial electron transport chain that affect ROS production [24–27]. In this regard, rotenone is a pesticide that induces symptoms similar to PD in animal models, and it has been suggested to increase the risk of PD in humans as well [25]. This substance is a naturally occurring ketone derived from the roots of tropical leguminous plants, which rapidly crosses the cell membranes and act as an inhibitor of complex I of the respiratory chain, that causes degeneration of dopaminergic neurons and motor dysfunction associated with PD. Furthermore, rotenone neurotoxicity is also associated with increased ROS generation and mitochondrial dysfunction [1, 24–26, 28–30]. In the present study, we assessed the possible protective effects of the nicotine analogs (*E*)-nicotinaldehyde O-cinnamyloxime, and 3-(pyridin-3-yl)-3a,4,5,6,7,7a-hexahidrobenzo[d]isoxazole on the dopaminergic SH-SY5Y cell line subjected to rotenone by modulating cell survival and ROS production.

Materials and Methods

Computational Studies

First, all of the analogs' structures were drawn by Avogadro using MMFF force and it was ensured that chirality is correct. The calculations were carried out using the Gaussian09 program package using dispersion-corrected *B3LYP* level of theory and cc-PVDZ basis set. In order to find the minimum energy conformation, eight analogs and nicotine were optimized at the DFT B3LYP/6-31G level, and later, a semi-empirical PM6 level conformational analysis was carried out on the rotations. The minimum energy conformation found for the analogs was used as the initial model for the optimization. No imaginary vibrational frequencies were found at the optimized geometries, indicating that they are true minima of the potential energy surface.

Preparation of Nicotine and Its Analogs for Docking

Our laboratory initially had a list of different nicotine analogs presenting varied structural conformations, of which two presented the possible best interaction with the nicotinic receptor (see methods below). In this regard, a series of three molecules were employed in the present study: two nicotine analogs and nicotine. The chemical structures are shown in Fig. 1. The initial structures of these compounds were sketched on ACD/ChemSketch and energetically minimized using the OPLS 2005 force field, with a charge located on the nitrogen of the pyrrole cycle. Structure of nicotine was retrieved from the Protein Data Bank and sketched and minimized using the Epik method in Maestro 9.5.

Structure Refinement and Molecular Docking

The initial structure of nAChR α7 was taken from the crystal structure of the ligand-binding domain of a pentameric Alpha7 nicotinic receptor complexed with epibatidine at 3.10 Å (PDB: 3SQ9). The water molecules and the epibatidine were removed and hydrogens were added to the system.

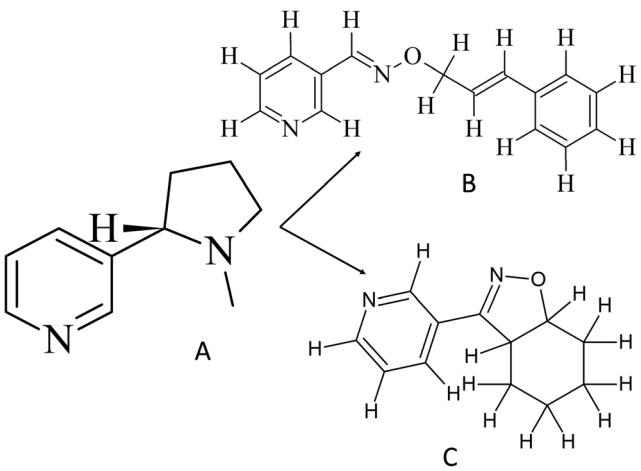

Fig. 1 Nicotine and nicotine analogs used in our study. **a** Nicotine; **b** (E)-nicotinaldehyde O-cinnamyl oxime (analog 1); **c** 3-(pyridin-3-yl)-3a,4,5,6,7,7a-hexahidrobenzo[d]isoxazole (analog 2)

A putative binding pocket was determined according to the published result of [31]). In this paper, the authors generated a series of chimeras by combining the sequences from α7 with those from Acetylcholine binding protein (AChBP), and the final construct shared 64% of sequence identity and had 71% similarity with native α7 [31]. The pocket is situated in the extracellular side of the neuron with residues from loops A–C of the principal subunit and loops D–E of the complementary subunit. The cavity is mainly composed of the conserved residues Tyr91 from loop A, Trp145 from loop B, Tyr184 and Tyr191 from loop C, Trp53 from loop D, and Leu106, Gln114 and Leu116 from loop E.

The geometry of the receptor was optimized using the MM2 molecular mechanic force field of the MAESTRO molecular modeling package (Maestro, version 9.5, Schrödinger). The effect of ionization states of docked compounds to the binding scores has been previously reported [32]. Since ionization states of docked compounds have not yet been determined experimentally, the neutral and ionized states (aliphatic amine and carboxylic acid groups of compounds to be docked) were protonated and deprotonated separately.

Before docking, conformational analysis was applied to the ligands using the Maestro 9.5. This option locates the minimal energy available for a set of molecules, stored in a database by randomly perturbing torsions, minimizing, and eliminating the duplicates. The maximum number of conformers for each molecule was set to 30 and the top 10 lowest energy conformers were used in docking simulations, and only the best docked complex was considered for further analysis.

The advanced molecular docking program AutoDockVina 1.1.2 [33], which uses a powerful Lamarckian genetic algorithm (LGA) method for conformational search and docking, was applied for the automated molecular docking simulations [34]. Briefly, the LGA described the relationship between the antagonists and the receptors by the translation, orientation, and conformation of the antagonists and can handle ligands with more degrees of freedom than other methods, being the most efficient, reliable, and successful [34]. The whole docking scheme could be stated as follows:

First, the receptor molecules were checked for polar hydrogen and assigned for partial atomic charges, the PDBQS file was created, and the nicotine analogs were coupled in the interface between 2 α subunits, focusing grid: 31.216 in *X*-axis, 4.296 in *Y*-axis, and 8.615 in *Z*-axis. The size of the grid box was 16 in X, Y, and Z and was used as a spacing of 1 Å between grid points in the ligand-binding site. A series of the docking parameters were set on. The atom types, generations, and the run numbers for LGA algorithm were properly assigned according to the requirement of the Amber force field. Free energy scores for ligands were calculated using the scoring function in Autodock, and finally, the docked complexes of analogs–receptor were selected according to the criteria of interacting energy combined with geometrical matching quality. These complexes were used as the starting conformation for further energetic minimization and geometrical optimization before the final binding models were achieved.

Experimental Studies

Cell Cultures

Human neuroblastoma-derived cell line SH-SY5Y (Code ATCC CRL-2266) was grown on 75-cm^2 culture dishes, in DMEM/F12 medium (Sigma®) supplemented with 10% fetal bovine serum (FBS) and 1% antibiotic-antimycotic Lonza® solution of penicillin/streptomycin (10 U penicillin/10 μg streptomycin/25 ng amphotericin). Cells were incubated at 37 °C, 5% CO_2, and 95% of air (*v*/*v*). The medium was removed and replaced every 2 days and subcultures were made every 7 days. These cells have adrenergic phenotype, express dopaminergic markers, and have been widely used in PD studies [24–26, 28–30].

Chemistry

Synthesis of (*E*)-nicotinaldehyde*O*-Cinnamyloxime (1) and 3-(Pyridin-3-yl)-3a,4,5,6,7,7a-Hexahidrobenzo[d]Isoxazole (2)

Compounds 1 and 2 (Fig. 1) were synthetized using standard procedures employed in the laboratory of organic synthesis at Pontificia Universidad Javeriana [35]. All used reagents and solvents were purchased from Sigma-Aldrich and J.T. Baker and used as received. NMR spectra were acquired in a Bruker Avance spectrometer operating at 300 MHz (^{1}H) and 75 MHz (^{13}C). LR-MS analyses were performed in an Agilent 6850 series II, coupled to a mass spectrometer Agilent 5975B VL (EI, 70 eV).

A mixture of nicotinaldoxime (0,200 g, 1.64 mmol) and NaOH (0.131 g, 3.28 mmol) in acetone (2.3 mL) was refluxed during 30 min. After this time, cinnamil bromide (0.37 g, 1.80 mmol) was added and the resulting mixture was refluxed during 3 h. The reaction was quenched by the addition of acetic acid, extracted with ethyl acetate, and dried with Na_2SO_4. The organic solvents were evaporated at low pressure and the residue was chromatographed using silica-gel 130–270 mesh and eluted with 10% ethyl acetate/hexane to yield the compound (*E*)-nicotinaldehyde *O*-cinnamyl oxime as a yellow oil (293 mg, 75%).

^{1}H NMR (300 MHz, $CDCl_3$) δ 4.88 (dd, J = 6.4, 1.3 Hz, 2H, OCH_2), 6.44 (dt, J = 15.9, 6.3 Hz, 1H, PhCH = C<u>H</u>), 6.72 (dt, J = 15.9, 1.4 Hz, 1H, PhC<u>H</u> = CH), 7.40–7.24 (m, 4H, H-5 Py, H-3,4,5 Ar), 7.49–7.41 (m, 2H, H-2,6 Ar), 8.00 (dt, J = 8.0, 2.0 Hz, 1H, H-4 Py), 8.16 (s, 1H, CH = NO), 8.62 (dd, J = 4.8, 1.7 Hz, 1H, H-6 Py), 8.77 (dd, J = 2.2, 0.8 Hz, 1H, H-2 Py). **^{13}C NMR** (75 MHz, $CDCl_3$) δ, 75.30 (OCH_2), 123.65

(C-5 Py), 124.72(CH = CHPh), 126.62 (C-2,6 Ar), 127.95(C-4 Ar), 128.33(C-3 Py), 128.60(C-3,5 Ar), 133.48(C-4 Py), 133.83 (CH = CHPh), 136.47(C-1 Ar), 145.89 (C = NO), 148.75 (C-2 Py), 150.67 (C-6 Py). **LR-MS (EI)**, m/z (I_{rel}, %): 238.1 $[M]^+$ (6).

3-(Pyridin-3-yl)-3a,4,5,6,7,7a-Hexahidrobenzo[d]Isoxazole (2) A mixture of nicotinaldoxime (0.122 g, 1.0 mmol) and cyclohexene (0.166 g, 2.0 mmol) in CH_2Cl_2 (4 mL) was cooled and stirred in an ice bath. A 5.25% aqueous solution of NaOCl (4 mL, 2.8 mmol) was added dropwise and the resulting mixture was stirred during 3 h. The reaction mixture was extracted with CH_2Cl_2, dried with Na_2SO_4, and the organic solvents were evaporated at low pressure. The residue was chromatographed using silica gel 230–400 mesh and eluted with 10% ethyl acetate/hexane to yield compound 3-(pyridin-3-yl)-3a,4,5,6,7,7a-hexahydrobenzo[d]isoxazole as a brown oil (121 mg, 60%).

^{1}H NMR spectrum, δ, ppm (J, Hz): (300 MHz, $CDCl_3$) δ 1.11–1.27 (m, 2H, H-4eq, H-5ax), 1.50–1.62 (m, 1H, H-6eq), 1.64–1.73 (m, 2H, H-5eq, H-6ax), 1.76–1.85 (m, 1H, H-7eq), 1.97–2.06 (m, 1H, H-4ax), 2.30 (dm, J = 15.2, 1H, H-7ax), 3.32 (td, J = 9.9, 7.2 Hz, 1H, 3a), 4.55 (dt, J = 7.2, 3.4 Hz, 1H, 7a), 7.36 (ddd, J = 8.0, 4.8, 0.9 Hz, 1H, H-5 Py), 8.10 (ddd, J = 8.0, 2.2, 1.7 Hz, 1H, H-4 Py), 8.64(dd, J = 4.8, 1.7 Hz, 1H, H-6 Py), 8.87(d, J = 2.0 Hz, 1H, H-2 Py), **^{13}C-NMR** (75 MHz, CDCl3) δ, 20.1(C-6), 22.1 (C-5), 24.9 (C-7), 26.2 (C-4), 43.6 (C-3a), 80.9 (C-7a), 123.7 (C-5 Py), 125.7(C-3 Py), 134.2(C-4 Py), 148.0(C-2 Py), 150.7(C-6 Py), 161.5 (C-3 Isoxazole). **LR-MS (EI)**, m/z (I_{rel}, %): 202.1 $[M]^+$ (100).

Treatment Preparation

Nicotine and nicotine analogs were diluted in dimethyl sulfoxide (DMSO) to 100% before being diluted in FBS-free culture medium. For biological assays, the final concentrations of nicotine and nicotine analogs were 1, 10, 50, and 100 μM. In control group, DMSO was added to the FBS-free culture medium. Rotenone assays were made to determine the IC_{50} of this pesticide, i.e., time and concentration wherein the substance produced cell death in 50% of cells, in order to obtain time and concentration of treatment with rotenone for use in next bioassays. With Y = 100/(1 + 10^ ((X-LogIC^{50})) formula, GraphPad Prism 5 determined the rotenone IC_{50} at 24 h of treatment. In every assay, we used DMSO (0.01%) as control (which was the solvent where analogs were diluted) at a concentration of 0.01%.

Cell Viability Assays

Cell viability was tested using 3-(4,5-dimethylthiazol-2-yl)-2,5-diphenyltetrazolium bromide (MTT) assay (Sigma, St Louis, Missouri, USA). These assays were performed to determine the concentration at which nicotine analogs were toxic and discard that concentration in following assays and to determine rotenone IC_{50}. Additionally, we established which were the best protective conditions of the nicotine analogs against rotenone (co-treatment, pre-treatment, or post-treatment) (Suppl. Material). Cells were seeded into 96-well plates in DMEM/F12 culture medium containing 10% bovine fetal serum at seeding density of 20,000 cells per well, incubated for 36 h until they reach confluence. After this period of time, medium was removed and replaced with FBS-free medium. This was performed to avoid an experimental error where cell viability was influenced by serum and not by nicotine analogs. Cells were left without FBS for 12 h, and subsequently, cells were treated according to different experimental paradigms. Viability was assessed and standardized at 24, 48, and 72 h, following treatment with nicotine or nicotine analogs (1, 10, and 100 μM), and with rotenone (1, 10, 50, and 100 μM), by adding MTT solution at the final concentration of 5 mg/mL for 4 h at 37 °C in order to allow the formation of formazan crystal. The cells were then lysed by the addition of DMSO. The blue formazan product was evaluated in a plate reader at 595 nm, and then, the values were normalized to the value of control cultures without treatment, which was considered as 100% survival. Each assay was performed with a minimum of eight replicate wells for each condition. In addition, cells were stained with propidium iodide (PI, 50 μg/mL) and cell viability was assessed through flow cytometry.

Determination of Reactive Oxygen Species

ROS production was evaluated by flow cytometry. Briefly, cells were seeded at a density of 100,000 cells per well into 24-well plates in DMEM/F12 culture medium containing 10% FBS and were then treated according to each experimental paradigm in the next day. To measure the effect of nicotine and nicotine analogs on superoxide anions (O_2^-) and hydrogen peroxide (H_2O_2) production, cells were treated in the dark at 37 °C for 30 min with 5 μM dihydroethidium (DHE; Sigma) or 10 μM 2′,7′–dichlorofluorescein diacetate (DCFDA), respectively. The cells were then washed in PBS and trypsinized (Trypsin/EDTA 500 mg/L: 200 mg/L-LONZA, Walkersville, USA) for flow cytometry analysis. Cells were analyzed in a Guava EasyCyte™ (Millipore, Billerica, Massachusetts, USA) cytometer. Each assay was performed with a minimum of six replicates for each condition. The experiment was repeated three times.

Statistical Analysis

Data obtained from this study were tested for normal distribution using Kolmogorov-Smirnov test and for homogeneity of variance using Levene's test. Data were then examined by one-way analysis of variance (ANOVA), followed by

Dunnett's post hoc test for comparisons between controls and treatments and Tukey's post hoc test for multiple comparisons between the means of treatments and time points. Data are presented as mean ± SEM of three independent experiments. A statistically significant difference was defined at $p < 0.05$.

Results

Determination of the Best-Docked Nicotine Analog-α7-nAChR Binding Interaction

It is important to point that we initially used computational tools to address whether nicotine analogs bind to α7-nAChR as similar as to the endogenous molecule, nicotine. In this regard, the structures of the nicotine analogs that were built and modeled in ACD/ChemSketch are shown in Fig. 1, along with the nicotine structure. These models were validated in Maestro 9.5, which yielded the most stable structure with the lowest free energy of each nicotine analogs using the OPLS2005 field force (Fig. 2a, b). Later, these structures were used in the simulation of the ligand-receptor interaction. The crystallographic structure of the α7-nAChR ligand binding domain (PDB: 3SQ9) was obtained from the Protein Data Bank (Fig. 3).

There is a ligand-binding site in each of the five interfaces between the subunits of the pentameric structure of α7-nAChR [32]; therefore, the grid box was centered precisely on one of those interfaces when using Autodock Vina 1.1.2. The binding free energy function had a period of desolvation (removing a solvent from a material in solution) that calculates the impact of the dissolvent in the binding with the ligand [32]. To validate the coupling results, the binding free energy obtained with the nicotine analogs was compared with that of the nicotine molecule. This molecule was obtained from the X-ray structure of the binding complex between nicotine and the acetylcholine binding protein (AChBP) (PDB: 1UW6) and was re-coupled on the previously obtained structure of the α7-nAChR ligand binding domain.

To explore the binding mode of the nicotine analogs to the α7-nAChR, they were examined in the first instance in the solvent accessible surface areas, on the interfaces of the receptor close to the ligand binding sites. In the structure of the α7-nAChR ligand-binding domain, the conserved residues form a narrow hydrophobic pocket. Analogs 1 and 2 were coupled to the α7-nAChR (PDB: 3SQ9). Nine best conformations of each ligand were settled through Autodock Vina 1.1.2 with

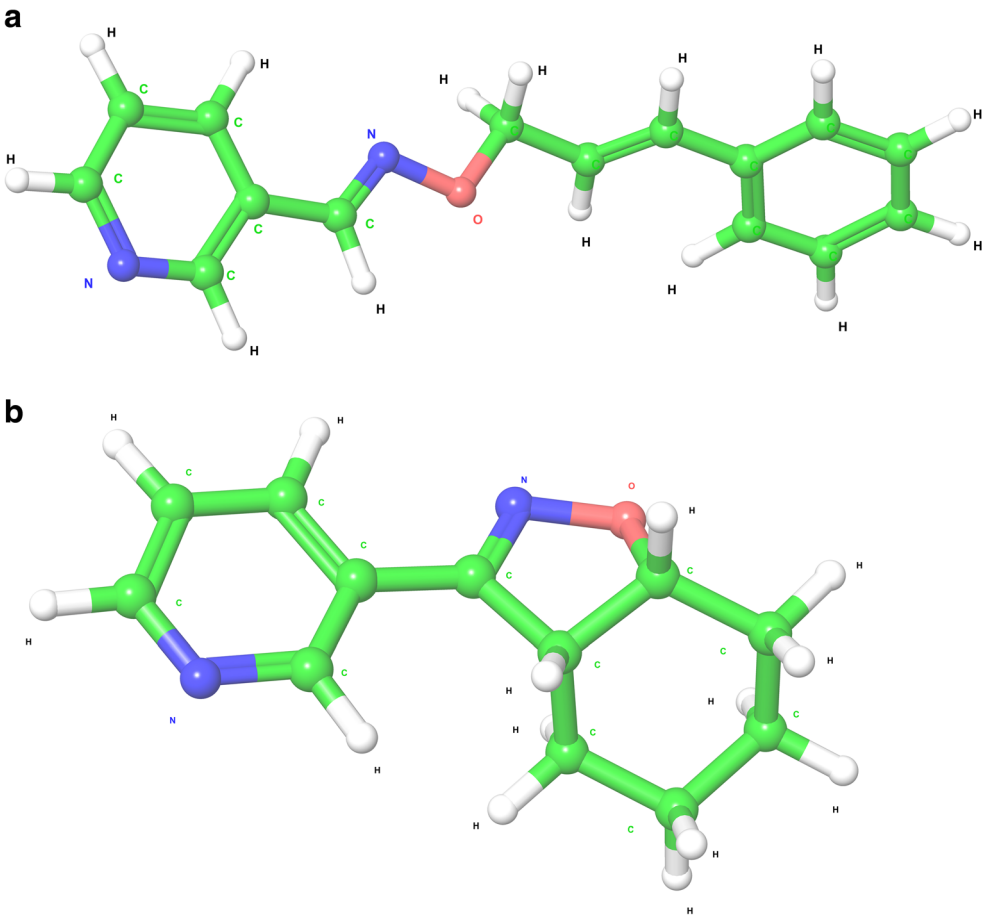

Fig. 2 Nicotine analogs with the most stable structure and lower free energy assessed by Maestro 9.5. **a** Analog 1, **b** analog 2

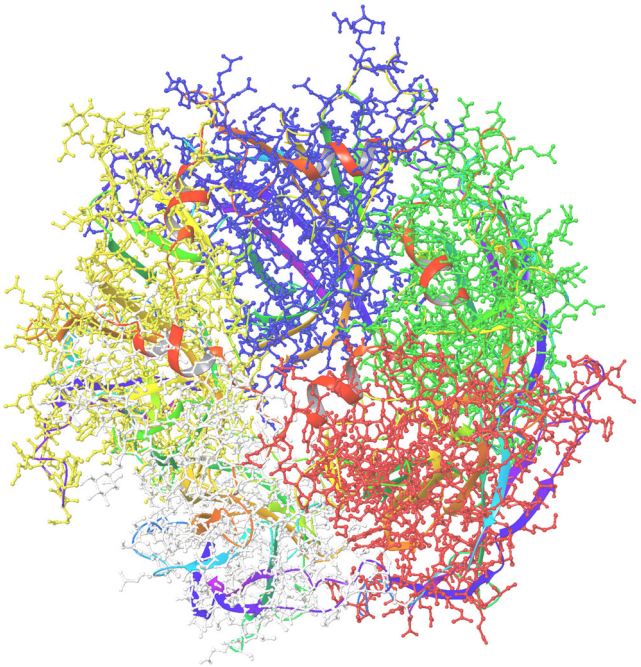

Fig. 3 3D structure of α7 nAChR ligand binding domain. Each of the five α subunits are displayed in different color

respect to the binding site on the receptor. The best of these conformations were chosen for constructing its schematic representation in Maestro 9.5.

The respective binding energies were also obtained with Autodock Vina (Table 1), which indicated that the two nicotine analogs had a minor binding energy relative to that of the nicotine molecule, thus demonstrating that these nicotine analogs were possibly interacting with the receptor with a higher affinity. The binding affinities of the two nicotine analogs studied with the binding site of the α7-nAChR are listed in Table 2 in relation to the binding site of the α7-nAChR, in units of the dissociation constant, which is used to describe the affinity between a ligand and its receptor. This constant defines how closely or strongly a ligand binds to a particular protein, and this affinity is influenced by the non-covalent intermolecular interactions existing between the two molecules, such as the hydrogen bonds, the electrostatic interactions, and the hydrophobic and Van der Waals forces [36, 37].

The resulting complexes of the binding of the best conformation of each of the nicotine analogs with the α7-nAChR ligand-binding domain are shown in Fig. 4. It was possible with Maestro 9.5 to obtain the receptor residues with which nicotine analogs interact in order to observe strong similarities and small differences (Fig. 4). The residues of the α7-nAChR binding site interacting with analog 1 were THR101, PRO97, VAL99, LYS96, PRO102, and GLN103. In the interaction between analog 2 and the α7-nAChR, the binding sites were implicated by the residues PRO79, SER81, GLN103, THR101, and PRO102. On the other hand, it was found that on the ligand binding site on the interface between 2 α subunits, the protonated amino groups of these ligands were bound to one of the α subunits and the other parts of the nicotine analogs were bound to the other α subunit. The coupling of analog 1 and 2 to α7-nAChR indicated that both compounds formed 2 hydrogen bonds with the receptor residues, and next, they will be tested in in vitro assays to address their possible protective actions.

Effect of Nicotine Analogs on Cell Viability

We assessed whether nicotine analogs affected SH-SY5Y cell viability under normal culture conditions. MTT cell viability assay indicated that analog 1 at the concentrations of 1 and 10 μM did not affect cell survival in any of the three evaluated timepoints (24, 48, and 72 h) when compared with the control group. However, a concentration of 100 μM of this nicotine analog decreased cell viability by 44.46 ±13.09% ($p < 0.05$) at 24 h and by 34.82 ±17.67% ($p < 0.05$) at 48 h (Suppl Fig. 1A). Otherwise, none of the analog 2 concentrations affected cell viability at 24 h. However, this nicotine analog at the concentration of 100 μM decreased cell viability by 40.17 ±17.37% ($p < 0.05$) at 48 h of treatment (Suppl Fig. 1B). On the other hand, we observed that 10 μM of this nicotine analog increased cell viability by 32.92 ±40.72% ($p < 0.05$) at 72 h (Suppl Fig. 1B).

Effect of Rotenone on Cell Viability

In the next experiment, we investigated the time and concentration at which rotenone caused 50% cell death, in order to use this timepoint and concentration in the subsequent assays. For this purpose, we performed a MTT cell viability assay

Table 1 Binding energies of nicotine analogs withα7-nAChR ligand-binding domain

Molecule	Affinity (kcal/mol)								
	1	2	3	4	5	6	7	8	9
(E)-nicotinaldehyde O-cinnamyl oxime (analog 1)	−4.2	−3.9	−3.8	−3.8	−3.8	−3.6	−3.5	−3.5	−3.5
3-(pyridin-3-yl)-3a,4,5,6,7,7a-hexahidrobenzo[d]isoxazole (analog 2)	−4.2	−4.1	−3.8	−3.8	−3.6	−3.5	−3.4	−3.3	−3.3
Nicotine	−3.3	−3.2	−3.2	−3.1	−3.0	−2.9	−2.9	−2.9	−2.8

Table 2 Binding affinities (K_i, nM) of analog 1, analog 2, and nicotine attached to α7-nAChR

Molecule	K_i (nM)
	α7
(E)-nicotinaldehyde O-cinnamyl oxime (analog 1)	1600
3-(pyridin-3-yl)-3a,4,5,6,7,7a-hexahidrobenzo[d]isoxazole (analog 2)	1900
Nicotine	3000

which showed that at 48 h, all rotenone concentrations (10, 100, and 200 μM) decreased cell viability relative to the control cells (39.04 ±43.54%, $p < 0.05$; 51.29 ± 17.01%, $p < 0.05$ and 70.12 ± 13.55%, $p < 0.05$, respectively). At 72 h, all concentrations of rotenone decreased cell viability by more than 50% relative to the control (79.08 ±6.295% ($p < 0.05$) by 10 μM, 81.31 ±8.68% ($p < 0.05$) by 100 μM, and 78.78 ±14.48% ($p < 0.05$) by 200 μM). We used these results to determine the rotenone IC_{50} at 48 h, because at 72 h, cell death was above 50%. For this procedure, we used GraphPad Prism 5 software [Y = 100/ (1 + 10^ ((X-Log IC_{50}))] and determined that IC_{50} after 24 h of treatment was 27.18 μM, a concentration that was approached to 30 μM in order to be used in the subsequent assays (Suppl Fig. 2).

Impact of Nicotine and Nicotine Analogs on the Viability of SH-SY5Y Cells Insulted with Rotenone

Next, we investigated if pre-treatment, co-treatment, or post-treatment with nicotine or nicotine analogs improved cell viability in rotenone-treated SH-SY5Y cells. Through the MTT assay, it was found that a 24-h pre-treatment with 1, 10, 50, and 100 μM of nicotine improved cell viability (Suppl Fig. 3) and a pre-treatment with 1 and 10 μM of analog 1 reduced cell death compared to the group of cells

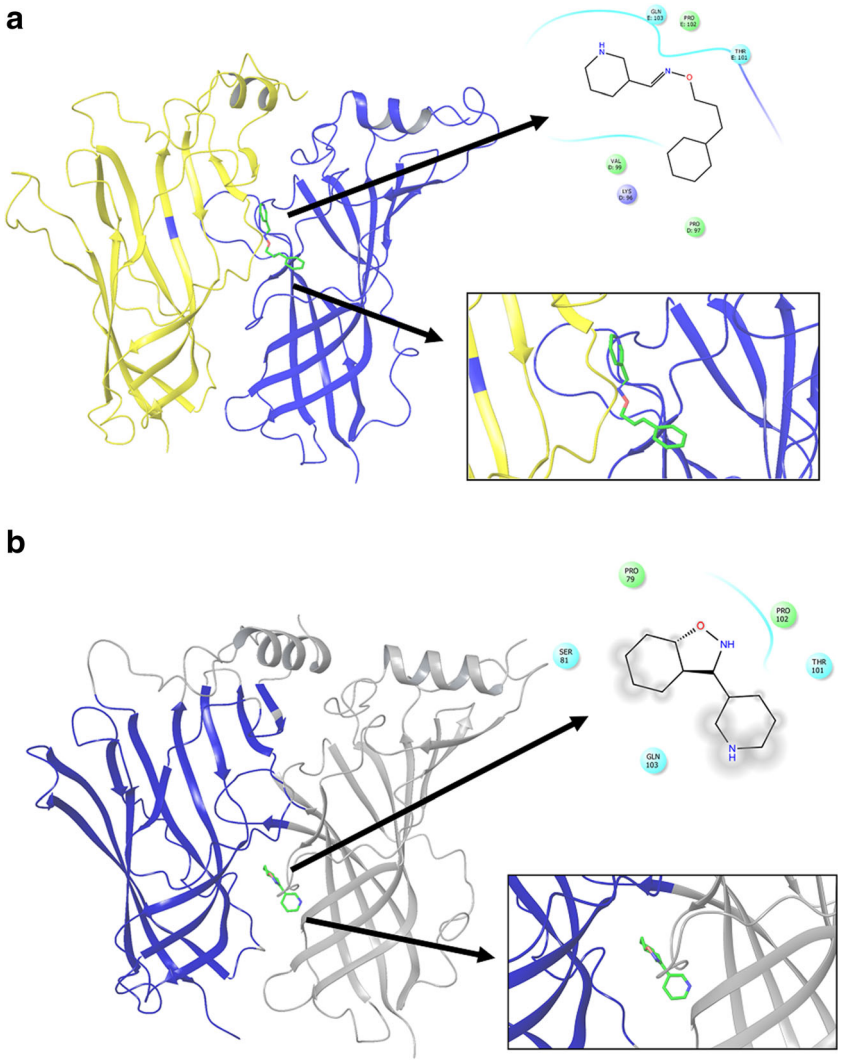

Fig. 4 Complexes resulting from the binding between the best conformation of each nicotine analog with α7 nAChR, and α7 nAChR residues that interact mainly with nicotine analogs evaluated in this research. **a** Analog 1; **b** analog 2

that were not pre-treated (Fig. 5a). Cells pretreated with 1 μM of analog 1 had an increased cell viability of 15.04 ±8.38% ($p < 0.0001$) compared with the rotenone-treated cells. In the same manner, cells pretreated with 10 μM of the analog 1 showed an average cell viability of 27.91 ±10.36% ($p < 0.0001$) greater than the non-pretreated cells (Fig. 5a). Thus, the 10-μM pretreatment with nicotine and the nicotine analog 1 was chosen to be used in the subsequent oxidative stress and ROS production experiments. It was observed that non-pretreated cells also had an abnormal morphology and were more likely to detach from the culture flask. None of the concentrations used in pre-treatments with analog 2 showed a significant difference in cell viability compared with the non-pretreated group of cells (Suppl Fig. 4).

Co-treatment with nicotine did not reduce cell death in SH-SY5Y cells insulted with rotenone at the IC_{50} dose (Suppl Fig. 5). Likewise, co-treatment with analog 1 (Suppl Fig. 6) or analog 2 (Suppl Fig. 7) did not reduce cell death in SH-SY5Y cells insulted with rotenone at the IC_{50} dose either. Moreover, post-treatment with nicotine did not reduce cell death in SH-SY5Y cells insulted with rotenone at the IC_{50} dose (Suppl Fig. 8). Neither post-treatment with analog 1 (Suppl Fig. 9) nor with analog 2 (Suppl Fig. 10) reduced the cell death in SH-SY5Y cells insulted with rotenone IC_{50}. Unexpectedly, post-treatment with 50 and 100 μM of analog 1 decreased cell viability by 9.024 ±9% ($p = 0.0024$) and 9.378 ±8.773% ($p = 0.0029$), respectively (Suppl Fig. 9).

To confirm if a pre-treatment with 1 and 10 μM of analog 1 was able to improve cell viability in SH-SY5Y cells insulted with rotenone at the IC_{50} dose, we conducted a flow cytometry assay with propidium iodide (Fig. 5b). Our results showed significant differences between the mean fluorescence intensity (MFI) of rotenone-treated cells pre-treated with 1, 10, and 50 μM concentrations of analog 1 and control cells. Pre-treated cells with analog 1 presented a lower MFI and therefore less cell death, confirming that these concentrations of this nicotine analog are capable of decreasing cell death. There was a MFI difference of 21.24 ±1.004% ($p = 0.0169$) between the cells that were not pre-treated and those pre-treated with 1 μM of analog 1, a difference of 24.5 ±2.479 ($p = 0.0173$) between the cells that were not pre-treated and those pre-treated with 10 μM, and a difference of 13.96 ±7.868% ($p = 0.0399$) between the cells that were not pre-treated and those pre-treated with 50 μM of the nicotine analog 1 (Fig. 5b). There were no significant differences between the cells pre-treated with 100 μM and the cells that were not pre-treated. Moreover, no significant differences were found between the MFI of cells pre-treated with 1, 10, and 50 μM of analog 1, showing that all of the three concentrations were equally beneficial in improving cell viability (Fig. 5b).

Oxidative Stress Assessment

Oxidative stress was assessed by flow cytometry using *dihydroethidium* (DHE) and 2′,7′-dichlorofluorescein diacetate (DCFDA) to measure the effect of pre-treatment with nicotine (10 μM) or analog 1 (10 μM) on the superoxide anion (O_2^-) and hydrogen peroxide (H_2O_2) production in SH-SY5Y cells insulted with rotenone at the IC_{50} dose. We observed that nicotine reduced O_2^- production by 66.43 ±26.45% ($p = 0.0061$) compared with the rotenone-treated cells. Moreover, pre-treatment with nicotine analog 1 was capable of reducing O_2^- production by 49.24 ±6.515% ($p = 0.0104$) compared with the non-pre-treated cells (Fig. 6a). There were no significant differences in ROS production between cells pre-treated with nicotine and those pre-treated with the nicotine analog 1. Additionally, we measured peroxide production by flow cytometry using 2′,7′-dichlorofluorescein diacetate (DCFDA). Both nicotine and the nicotine analog 1 were able to reduce peroxide production by 37.98±8.998% ($p = 0.0071$) and 54.06 ±6.455% ($p = 0.0132$), respectively. There was no significant difference in peroxide production between the cells pre-treated with nicotine and nicotine analog 1 (Fig. 6b). These combined results

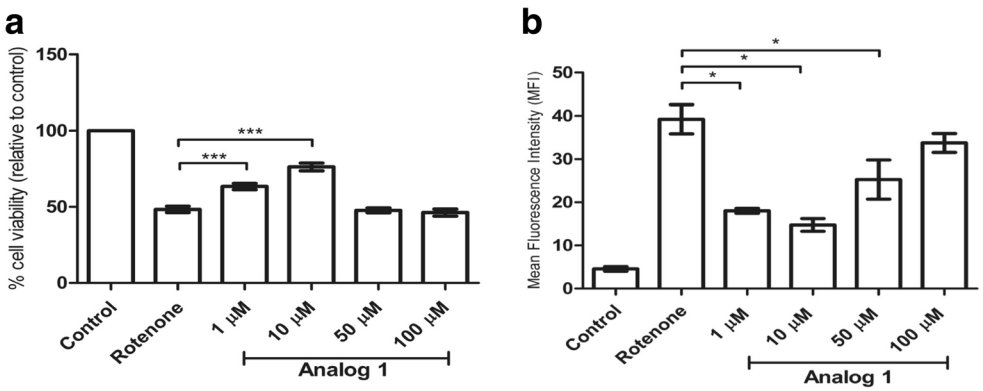

Fig. 5 The effect of a pre-treatment with analog 1 on cell viability. **a** Cell viability assay with MTT. Independent experiments were performed in triplicate. Results are presented as cell viability percentage and SEM. The effect of a pre-treatment with analog 1 (before the application of rotenone IC_{50} (30 μM)) on cell viability was confirmed in SH-SY5Y cells through flow cytometry with propidium iodide (**b**). Independent experiments were performed in triplicate. Results are presented as the mean fluorescence intensity (MFI) and SEM

suggested that nicotine analog 1 was able to reduce ROS production in an in vitro PD model, imitating the action of nicotine, and decreasing oxidative stress and cell death (Fig. 6).

Discussion

Nicotine analogs may play an important role in preventing or reducing the deleterious effects caused by excessive ROS production during PD development [24, 38]. This role might be due to their actions on mitochondria and their antioxidant properties that reduce the disruptive effects of oxidative stress in the CNS. Moreover, nicotine and its analogs are useful in eliminating excessive H_2O_2 and forming nicotine-pirroliniloxide groups or complexes with iron through the pyridine nitrogen [38]. It has been demonstrated that nicotine analogs and other α7 nAChR agonists could exert neuroprotective effects [12, 39]. On the other hand, nicotine produces dependence and acts as a toxic agent that damages cells and tissues in the human body. For this reason, we assessed the possible beneficial effect produced by two synthetic nicotine analogs not previously studied, (*E*)-nicotinaldehyde O-cinnamyl oxime (analog 1) and 3-(pyridin-3-yl)-3a,4,5,6,7,7a-hexahidrobenzo[d]isoxazole (analog 2), on cell viability and oxidative stress in SH-SY5Y cells insulted with rotenone. Initially, we conducted a molecular docking study between nicotine analogs and α7-nAChR. Molecular docking studies are very useful for understanding the interactions between ligands and putative receptors that could be useful in the research of novel therapeutic compounds [40, 41]. According to our results, the binding free energy of both nicotine analogs was lower than that of nicotine, indicating a possible higher affinity for α7-nAChR. This fact suggests that the studied nicotine analogs require a lower concentration in comparison with the nicotine concentration required to achieve a beneficial effect on cell viability and ROS generation. Our results also showed that the most important residues in the interaction between the α7-nAChR binding site and both nicotine analogs were THR101, PRO102, and GLN103. Both nicotine analogs are neo-compounds for which there is no previous information on interaction with nAChRs. Interestingly, Dukat et al. [42] tested two nicotine analogs synthesized by a replacement at the position 5 of 5-bromonicotine and 5-metoxinicotine [42]. This study showed that both analogs had high affinity for nAChRs (although about 3 to 6 times lower than that of nicotine). Furthermore, other nicotine analogs that have been developed as nAChRs agonists for PD treatment have been able to exert neuroprotection, increase cell viability, and reduce ROS production and oxidative stress [17, 42]. As previously demonstrated by Yuan and Petukhov [32], an increase in the number of atoms connecting pyrrolidine and pyridine rings and an introduction of the alkyl substituent on the pyridine ring affect the binding and produce a change in the selectivity of these ligands to nAChRs [32]. Additionally, modeling studies performed by Yuan and Petukhov [32] coincide with the findings in our investigation with nicotine analogs. The ligands bind in the interface between the two neighboring subunits within the receptor, with the protonated amino group of nicotine analogs coupled in the conserved aromatic pocket of the receptor. Since these two nicotine analogs presented the best interaction with the nAChR α7 receptor, we hypothesized whether they could exert any protective effect in cells exposed to rotenone in vitro.

We performed experimental studies to assess the impact of synthetic analogs on cell viability and ROS production. Rotenone is considered as a useful tool for the study of PD in in vitro and in vivo models [24–26, 43]. It induces a chronic and systemic inhibition of complex I of the mitochondrial

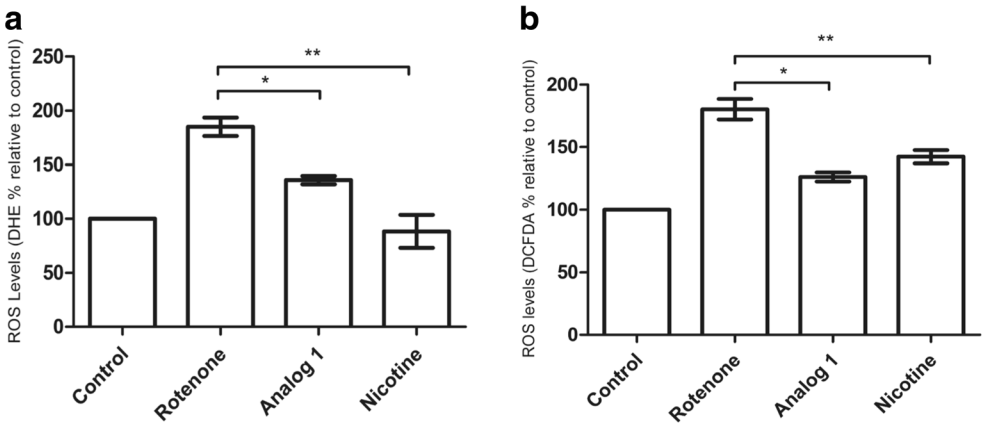

Fig. 6 The effect of a pre-treatment with nicotine or analog 1 on ROS production. **a** Superoxide anion levels using flow cytometry for DHE (*$p = 0.0104$, **$p = 0.0061$). **b** Hydrogen peroxide were assessed in SH-SY5Y cells by flow cytometry for DCFDA (*$p = 0.0132$, **$p = 0.0071$). Independent experiments were performed in triplicate. Results are presented as **a** the percentage of staining with DHE (ROS levels) relative to control, along with SEM, and **b** the percentage of staining with DCFDA (ROS levels) relative to control, along with SEM

respiratory chain and causes highly selective degeneration of nigrostriatal dopaminergic neurons followed by decreased ATP production and increased ROS production and oxidative stress, which ultimately lead to cell death [43, 44]. Nevertheless, according to Douna et al. [44], it was confirmed that it is the large amount of ROS production which causes cell death, and not the decreased ATP production [44]. Moreover, rotenone increases the generation of superoxide anions, which are highly toxic to cells as they allow the escape of electrons from complex I [38]. Rotenone has advantages over other neurotoxins such as MPTP and 6-OHDA in that it is capable of inducing accumulation of α-synuclein, which is among the PD hallmarks [44]. Additionally, we used SH-SY5Y cell line as it has a catecholaminergic phenotype and expresses nicotinic receptors [45].

Our results showed that IC_{50} dose of rotenone in SH-SY5Y cells was 30 μM at 24 h of treatment. This result differs from those reported by Nakamura et al. [46], who found that rotenone caused cell death in SH-SY5Y cells in a concentration-dependent and time-dependent matter and that rotenone IC_{50} was only 1 μM [46]. According to this study, rotenone acts in SH-SY5Y cells through degradation of caspases 3 and 9, after which a cleavage of the poly (ADP-ribose) polymerase occurs, leading to DNA fragmentation and cell death [46]. In the present study, only analog 1 at the concentrations of 1 and 10 μM mimicked the beneficial action of nicotine and improved cell viability in rotenone-insulted cells. Experimental concentrations of 1 and 10 μM of analog 1 are similar to concentrations of nicotine used in previous studies that demonstrated same beneficial effects [45, 47–49]. For example, Peng et al. [47] found that 40 μM of nicotine, a dose much higher than used in our study, protected primary cultures of mice dopaminergic neurons, thus increasing cell viability by 57% when compared with untreated cells [47]. Furthermore, Riveles et al. [45] found that concentrations of nicotine between 0.1 and 10 μM protected the SH-SY5Y cells against the toxic effects of 6-OHDA [45]. Indeed, Quik et al. [48, 50] showed that nicotine administration exerted partial neuroprotection against 6-OHDA and MPTP in rats, mice, and primates [48, 50]. Finally, Takeuchi et al. [49] demonstrated that nicotine pre-treatment protected the striatum and *substantia nigra* of rotenone-treated mice [49]. The ability of analog 1 to increase the cell viability in our PD model with rotenone could be due to the action of a signaling pathway hypothesized by Shimohama [51], where α7nAChR is activated and in turn stimulates the Src family, which activates the phosphatidylinositol 3 kinase (PI3K) and phosphorylates Akt. Once phosphorylated, Akt transmits a signal causing an upregulation of Bcl-2 and Bcl-x. According to Shimohama [51], this upregulation could prevent neuronal death caused by rotenone [51]. Therefore, the PI3K-Akt cascade contributed to the neuroprotective effect of nicotine (and probably of its analogs), and the Bcl-2 family was subsequently activated working as a factor that prevented neuronal death caused by rotenone. Moreover, Takeuchi et al. [49] found that PI3K-Akt/PKB inhibitors blocked the neuroprotective effects of nicotine in primary cultures of dopaminergic neurons exposed to rotenone [49], thus confirming Shimohama hypothesis and demonstrating that rotenone-induced toxicity is inhibited by α4β2 nAChR activation or by activation of the signaling pathway that involves α7 receptor and PI3K-Akt/PKB [51]. These researchers found that rotenone toxicity and nicotine neuroprotection occurred mostly after 24 h of treatment, similar to what we observed in our research where a 24-h pre-treatment with analog 1 showed neuroprotection and the highest rotenone toxicity was reached 24 h after this pre-treatment. However, further experiments are needed in order to identify the signaling pathways activated by nicotine analog 1 that confer protection against rotenone in SH-SY5Y cells.

Another hypothesis suggests that nicotine and some of its analogs are able to increase the number of nAChRs in the brain, thereby exerting neuroprotection. According to Peng et al. [52], nicotine upregulates the α3 nAChR (by 500–600%) and α7 nAChR (by 30%) in SH-SY5Y cells, and nicotine EC_{50} values required for an upregulation of α3 and α7 receptors in SH-SY5Y cells were 100 and 65 μM, respectively [47]. NAChR upregulation and increased cell viability were achieved after 24 h of treatment. Further research could be important to determine if increased cell viability caused by analog 1 in SH-SY5Y cells is accompanied by an increase in the number of nAChR receptors.

It is possible that nicotine and its analogs could prevent or delay the onset of PD through other signaling cascades. For example, nAChR activation by nicotine or its analogs triggers the release of dopamine and is involved in the neural modulation of inflammation. On the other hand, this anti-inflammatory mechanism involves a decrease in tumor necrosis factor α (TNF-α) and inducible nitric oxide synthase (iNOS) synthesis, which contribute to the neuroprotective effects of nicotine [12]. This anti-inflammatory action should be further investigated in future studies. It is also important to investigate the in vitro and in vivo PD models and other neuroprotective pathways such as those related to the activities of monoamine oxidases A and B (MAO-A and MAO-B), which decreases by nicotine treatment. This decrease in MAO activity causes a decrease in dopamine oxidation [53]. It is also probable that nicotine and its analogs could exert neuroprotection of dopaminergic neurons by stimulating the liberation of fibroblast growth factor-2 (FGF-2) [12].

Given that in PD, there is an increase of ROS, we investigated the antioxidant potential of analog 1 against rotenone-induced ROS generation. It was found that 10 μM of this nicotine analog had the capacity of reducing superoxide anion (DHE assay) and hydrogen peroxide (DCFDA assay) production in SH-SY5Y cells insulted for 24 h with rotenone at the IC_{50} dose. This finding is consistent with several studies that

have shown that nicotine is capable of decreasing superoxide anion generation and reducing oxidative stress by affecting the Fenton reaction [38, 54].

In conclusion, our results demonstrate that nicotine and nicotine analogs may protect SH-SY5Y cells against the rotenone insult, possibly through the activation of antioxidative elements and counterbalancing oxidative stress. However, additional studies are needed in order to deeply understand the mechanisms and the signaling pathways activated by nicotine and its analogs.

Acknowledgments This work was supported by Pontificia Universidad Javeriana (PUJ grants # 6337 and 6701) to GEB.

Compliance with Ethical Standards

Conflict of Interest The authors declare that they have no conflict of interest.

References

1. Kim HJ, Park HJ, Park HK, Chung JH (2009) Tranexamic acid protects against rotenone-induced apoptosis in human neuroblastoma SH-SY5Y cells. Toxicology 262(2):171–174
2. Barreto GE, Iarkov A, Moran VE (2014) Beneficial effects of nicotine, cotinine and its metabolites as potential agents for Parkinson's disease. Front Aging Neurosci 6:340
3. Barreto GE, Yarkov A, Avila-Rodriguez M, Aliev G, Echeverria V (2015) Nicotine-derived compounds as therapeutic tools against post-traumatic stress disorder. Curr Pharm Des 21(25):3589–3595
4. Echeverria V, Grizzell JA, Barreto GE (2016a) Neuroinflammation: A therapeutic target of cotinine for the treatment of psychiatric disorders? Curr Pharm Des 22(10):1324–1333
5. Echeverria V, Yarkov A, Aliev G (2016b) Positive modulators of the alpha7 nicotinic receptor against neuroinflammation and cognitive impairment in Alzheimer's disease. Prog Neurobiol 144:142–157
6. Grizzell JA, Patel S, Barreto GE, Echeverria V (2017) Cotinine improves visual recognition memory and decreases cortical tau phosphorylation in the Tg6799 mice. Prog Neuro-Psychopharmacol Biol Psychiatry 78:75–81
7. Jurado-Coronel JC, Avila-Rodriguez M, Capani F, Gonzalez J, Moran VE, Barreto GE (2016) Targeting the nicotinic acetylcholine receptors (nAChRs) in astrocytes as a potential therapeutic target in Parkinson's disease. Curr Pharm Des 22(10):1305–1311
8. Mendoza C, Barreto GE, Iarkov A, Tarasov VV, Aliev G, Echeverria V (2018) Cotinine: A therapy for memory extinction in post-traumatic stress disorder. Mol Neurobiol
9. Perez-Urrutia N, Mendoza C, Alvarez-Ricartes N, Oliveros-Matus P, Echeverria F, Grizzell JA, Barreto GE, Iarkov A et al (2017) Intranasal cotinine improves memory, and reduces depressive-like behavior, and GFAP+ cells loss induced by restraint stress in mice. Exp Neurol 295:211–221
10. Ye SQ, Zhou XY, Lai XJ, Zheng L, Chen XQ (2009) Silencing neuroglobin enhances neuronal vulnerability to oxidative injury by down-regulating 14-3-3gamma. Acta Pharmacol Sin 30(7):913–918
11. Quik M, Huang LZ, Parameswaran N, Bordia T, Campos C, Perez XA (2009) Multiple roles for nicotine in Parkinson's disease. Biochem Pharmacol 78(7):677–685
12. Ward RJ, Lallemand F, de Witte P, Dexter DT (2008) Neurochemical pathways involved in the protective effects of nicotine and ethanol in preventing the development of Parkinson's disease: Potential targets for the development of new therapeutic agents. Prog Neurobiol 85(2):135–147
13. Benowitz NL (2009) Pharmacology of nicotine: Addiction, smoking-induced disease, and therapeutics. Annu Rev Pharmacol Toxicol 49:57–71
14. Bolchi C, Valoti E, Gotti C, Fasoli F, Ruggeri P, Fumagalli L, Binda M, Mucchietto V et al (2015) Chemistry and pharmacology of a series of Unichiral analogues of 2-(2-Pyrrolidinyl)-1,4-benzodioxane, Prolinol phenyl ether, and Prolinol 3-Pyridyl ether designed as alpha4beta2-nicotinic acetylcholine receptor agonists. J Med Chem 58(16):6665–6677
15. Deng CB, Li J, Li LY, Sun FJ (2016) Protective effect of novel substituted nicotine hydrazide analogues against hypoxic brain injury in neonatal rats via inhibition of caspase. Bioorg Med Chem Lett 26(13):3195–3201
16. Pogocki D, Ruman T, Danilczuk M, Danilczuk M, Celuch M, Walajtys-Rode E (2007) Application of nicotine enantiomers, derivatives and analogues in therapy of neurodegenerative disorders. Eur J Pharmacol 563(1–3):18–39
17. Rao TS, Sacaan AI, Menzaghi FM, Reid RT, Adams PB, Correa LD, Whelan KT, Vernier JM (2004) Pharmacological characterization of SIB-1663, a conformationally rigid analog of nicotine. Brain Res 1003(1–2):42–53
18. Wang J, Li X, Yuan Q, Ren J, Huang J, Zeng B (2012) Synthesis and pharmacological properties of 5-alkyl substituted nicotine analogs. Chin J Chem 30(12):2813–2818
19. Albarracin SL, Stab B, Casas Z, Sutachan JJ, Samudio I, Gonzalez J, Gonzalo L, Capani F et al (2012) Effects of natural antioxidants in neurodegenerative disease. Nutr Neurosci 15(1):1–9
20. Mazo NA, Echeverria V, Cabezas R, Avila-Rodriguez M, Tarasov VV, Yarla NS, Aliev G, Barreto GE (2017) Medicinal plants as protective strategies against Parkinson's disease. Curr Pharm Des 23(28):4180–4188
21. Sutachan JJ, Casas Z, Albarracin SL, Stab BR 2nd, Samudio I, Gonzalez J, Morales L, Barreto GE (2012) Cellular and molecular mechanisms of antioxidants in Parkinson's disease. Nutr Neurosci 15(3):120–126
22. Guo L, Li L, Wang W, Pan Z, Zhou Q, Wu Z (2012) Mitochondrial reactive oxygen species mediates nicotine-induced hypoxia-inducible factor-1alpha expression in human non-small cell lung cancer cells. Biochim Biophys Acta 1822(6):852–861
23. Ross GW, Petrovitch H (2001) Current evidence for neuroprotective effects of nicotine and caffeine against Parkinson's disease. Drugs Aging 18(11):797–806
24. Cabezas R, Avila MF, Gonzalez J, El-Bacha RS, Barreto GE (2015) PDGF-BB protects mitochondria from rotenone in T98G cells. Neurotox Res 27(4):355–367
25. Cabezas R, El-Bacha RS, Gonzalez J, Barreto GE (2012) Mitochondrial functions in astrocytes: Neuroprotective implications from oxidative damage by rotenone. Neurosci Res 74(2):80–90
26. Cabezas R, Vega-Vela NE, Gonzalez-Sanmiguel J, Gonzalez J, Esquinas P, Echeverria V, Barreto GE (2018) PDGF-BB preserves mitochondrial morphology, attenuates ROS production, and upregulates Neuroglobin in an astrocytic model under rotenone insult. Mol Neurobiol 55(4):3085–3095
27. Chung WG, Miranda CL, Maier CS (2007) Epigallocatechin gallate (EGCG) potentiates the cytotoxicity of rotenone in neuroblastoma SH-SY5Y cells. Brain Res 1176:133–142
28. de Oliveira DM, Barreto G, Galeano P, Romero JI, Holubiec MI, Badorrey MS, Capani F, Alvarez LD (2011) Paullinia cupana Mart. Var. Sorbilis protects human dopaminergic neuroblastoma SH-

SY5Y cell line against rotenone-induced cytotoxicity. Hum Exp Toxicol 30(9):1382–1391
29. de Oliveria DM, Barreto G, De Andrade DV, Saraceno E, Aon-Bertolino L, Capani F, Dos Santos El Bacha R, Giraldez LD (2009) Cytoprotective effect of *Valeriana officinalis* extract on an in vitro experimental model of Parkinson disease. Neurochem Res 34(2):215–220
30. Valverde GDAD, Madureira de Oliveria D, Barreto G, Bertolino LA, Saraceno E, Capani F, Giraldez LD (2008) Effects of the extract of Anemopaegma mirandum (Catuaba) on rotenone-induced apoptosis in human neuroblastomas SH-SY5Y cells. Brain Res 1198:188–196
31. Li SX, Huang S, Bren N, Noridomi K, Dellisanti CD, Sine SM, Chen L (2011) Ligand-binding domain of an alpha7-nicotinic receptor chimera and its complex with agonist. Nat Neurosci 14(10):1253–1259
32. Yuan H, Petukhov PA (2006) Computational evidence for the ligand selectivity to the alpha4beta2 and alpha3beta4 nicotinic acetylcholine receptors. Bioorg Med Chem 14(23):7936–7942
33. Trott O, Olson AJ (2010) AutoDock Vina: Improving the speed and accuracy of docking with a new scoring function, efficient optimization, and multithreading. J Comput Chem 31(2):455–461
34. Morris GM, Goodsell DS, Halliday RS, Huey R, Hart WE, Belew RK, Olson AJ (1998) Automated docking using a Lamarckian genetic algorithm and an empirical binding free energy function. J Comput Chem 19(14):1639–1662
35. Diaz-Velandia J, Durán-Díaz N, Robles-Camargo J, Loaiza A (2011) Synthesis and in vitro assessment of antifungal activity of oximes, oxime ethers and isoxazoles. Univ Sci 16(3):294–302
36. Minton AP (2001) The influence of macromolecular crowding and macromolecular confinement on biochemical reactions in physiological media. J Biol Chem 276(14):10577–10580
37. Zhou HX, Rivas G, Minton AP (2008) Macromolecular crowding and confinement: Biochemical, biophysical, and potential physiological consequences. Annu Rev Biophys 37:375–397
38. Cormier A, Morin C, Zini R, Tillement JP, Lagrue G (2003) Nicotine protects rat brain mitochondria against experimental injuries. Neuropharmacology 44(5):642–652
39. Prendergast MA, Harris BR, Mayer S, Littleton JM (2000) Chronic, but not acute, nicotine exposure attenuates ethanol withdrawal-induced hippocampal damage in vitro. Alcohol Clin Exp Res 24(10):1583–1592
40. Noha SM, Schmidhammer H, Spetea M (2017) Molecular docking, molecular dynamics, and structure-activity relationship explorations of 14-oxygenated N-Methylmorphinan-6-ones as potent mu-opioid receptor agonists. ACS Chem Neurosci 8(6):1327–1337
41. Shrivastava A, Kumar K, Prasad K (2017) Molecular docking studies: The success should overrule the doubts? Journal of Proteomics & Bioinformatics 10:202–206
42. Dukat M, Damaj IM, Young R, Vann R, Collins AC, Marks MJ, Martin BR, Glennon RA (2002) Functional diversity among 5-substituted nicotine analogs; in vitro and in vivo investigations. Eur J Pharmacol 435(2–3):171–180
43. Betarbet R, Sherer TB, MacKenzie G, Garcia-Osuna M, Panov AV, Greenamyre JT (2000) Chronic systemic pesticide exposure reproduces features of Parkinson's disease. Nat Neurosci 3(12): 1301–1306
44. Douna H, Bavelaar BM, Pellikaan H, Olivier B, Pieters T (2012) Neuroprotection in Parkinson's disease: A systematic review of the preclinical data. The Open Pharmacology Journal 6(1):12–26
45. Riveles K, Huang LZ, Quik M (2008) Cigarette smoke, nicotine and cotinine protect against 6-hydroxydopamine-induced toxicity in SH-SY5Y cells. Neurotoxicology 29(3):421–427
46. Nakamura K, Kitamura Y, Tsuchiya D, Inden M, Taniguchi T (2004) In vitro neurodegeneration model: Dopaminergic toxin-induced apoptosis in human SH-SY5Y cells. Int Congr Ser 1260(1):287–290
47. Peng J, Liu Q, Rao MS, Zeng X (2013) Using human pluripotent stem cell-derived dopaminergic neurons to evaluate candidate Parkinson's disease therapeutic agents in MPP+ and rotenone models. J Biomol Screen 18(5):522–533
48. Quik M, O'Neill M, Perez XA (2007) Nicotine neuroprotection against nigrostriatal damage: Importance of the animal model. Trends Pharmacol Sci 28(5):229–235
49. Takeuchi H, Yanagida T, Inden M, Takata K, Kitamura Y, Yamakawa K, Sawada H, Izumi Y et al (2009) Nicotinic receptor stimulation protects nigral dopaminergic neurons in rotenone-induced Parkinson's disease models. J Neurosci Res 87(2):576–585
50. Quik M, Bordia T, O'Leary K (2007) Nicotinic receptors as CNS targets for Parkinson's disease. Biochem Pharmacol 74(8):1224–1234
51. Shimohama S (2009) Nicotinic receptor-mediated neuroprotection in neurodegenerative disease models. Biol Pharm Bull 32(3):332–336
52. Peng X, Gerzanich V, Anand R, Wang F, Lindstrom J (1997) Chronic Nicotine Treatment Upregulates α3 and α7 Acetylcholine Receptor Subtypes Expressed by the Human Neuroblastoma Cell Line SH-SY5Y. Mol Pharmacol 51(1):776–784
53. Serres F, Carney SL (2006) Nicotine regulates SH-SY5Y neuroblastoma cell proliferation through the release of brain-derived neurotrophic factor. Brain Res 1101(1):36–42
54. Linert W, Bridge MH, Huber M, Bjugstad KB, Grossman S, Arendash GW (1999) In vitro and in vivo studies investigating possible antioxidant actions of nicotine: Relevance to Parkinson's and Alzheimer's diseases. Biochim Biophys Acta 1454(2):143–152